Mesoscale elements description of turbulent flow

A. A Burluka

School of Mechanical and Construction Engineering, Faculty of Engineering and Environment, Northumbria University, Newcastle-upon-Tyne NE1 8ST, UK

Abstract

This work proposes to describe a turbulent flow using a set of mesoscale elements, that is fluid elements of small, but finite, size the properties of which are representative of larger region surrounding them. Consideration of the fluid elements of finite dimensions allows one to formulate a small scale mixing model with an explicit dependency on the molecular transport coefficients. The dimensions of a mesoscale element are determined from an evolution equation accounting for the molecular diffusion and the strain rate induced by small-scale turbulence while its position is determined by convection by large-scale velocity components. In addition to consideration of the fluid elements of a finite size, the second key new concept is the notion of radius of influence over which such an element contributes to the statistics of the flow; this radius grows with time. It is shown that the proposed method satisfies the mass conservation and normalisation of the probability density functions of scalar quantities. The proposed method is illustrated with simulations of thermal mixing layer in grid turbulence.

Keywords: Turbulent mixing, Lagrangian description, Molecular transport,

Email address: alexey.burluka@northumbria.ac.uk (A. A Burluka)

1. Introduction

Common Lagrangian methods of description of a turbulent flow, see e.g. Pope [1], consider an ensemble of infinitesimally small fluid particles with Lagrangian marker typically taken as the the pair $(\boldsymbol{x}_0, t_0)$ of the position $\boldsymbol{x}_0$ at some initial time t_0. These particles travel within a continuous medium, often called fluid phase, and separate sets of equations governing the velocity, enthalpy or temperature, and other properties are formulated for these point particles and the continuous phase [1, 2]. The equations for the latter are Eulerian formulations of conservation laws in terms of partial differential equations written for fixed spatial locations. Application of such approach to a turbulent flow necessarily leads to unclosed terms in the governing equations for both Lagrangian particles and Eulerian continuum and the assumption that the Lagrangian particles are of zero size makes it impossible to include the action of molecular transport of mass or energy or momentum into the equations describing evolution of their properties. Owing to their zero size, the Lagrangian particles have zero mass and this causes difficulty in satisfying simultaneously normalisation of the probability density functions (pdf's) and conservation of mass [2].

Very commonly, the Lagrangian methods are applied to turbulent reacting flows where the average rate of a chemical reaction is found from averaging over the ensemble of the Lagrangian point particles, see e.g. Rowinski and Pope [3]. Crucial for this application, which is the main motivation for development of the present method, is the small-scale mixing model, i.e.

description of the mixing at the molecular level with the rate strongly increased by turbulence and a very large body of research has been devoted to this topic, see e.g. Dopazo [4] or Dopazo et al. [5] for a recent review. Yet, rather paradoxically, to the best of the author's knowledge, no small-scale mixing model has so far been formulated with an explicit account of the magnitude of the molecular transport coefficients while there is a large amount of evidence of importance of these coefficients [6, 7]. This work attempts development of a method which does bring into explicit consideration the coefficients of the molecular transport invoking consideration of Lagrangian elements of finite dimensions.

2. Mesoscale element method formulation

2.1. Basic principles

The mesoscale element (m.e.) is a moving parcel of the fluid with a fixed mass m_e which represents properties and influence of a much larger mass of fluid surrounding it. In that, the mesoscale method proposed here is a coarse-grained description of turbulence in Lagrangian frame. Dimensions of a mesoscale element are finite and, as discussed below, chosen opportunistically in the inertial interval of turbulence, in the range much smaller than characteristic flow dimension comparable with integral length scale of turbulence l_t. The idea behind the notion of small mesoscale element representing a larger flow region is that even though the latter may be composed of a large number of these small fluid elements it may be represented with only one or a few m.e. having a certain radius of influence going beyond their size. In this manner, the turbulent fluctuations of flow velocity and medium prop-

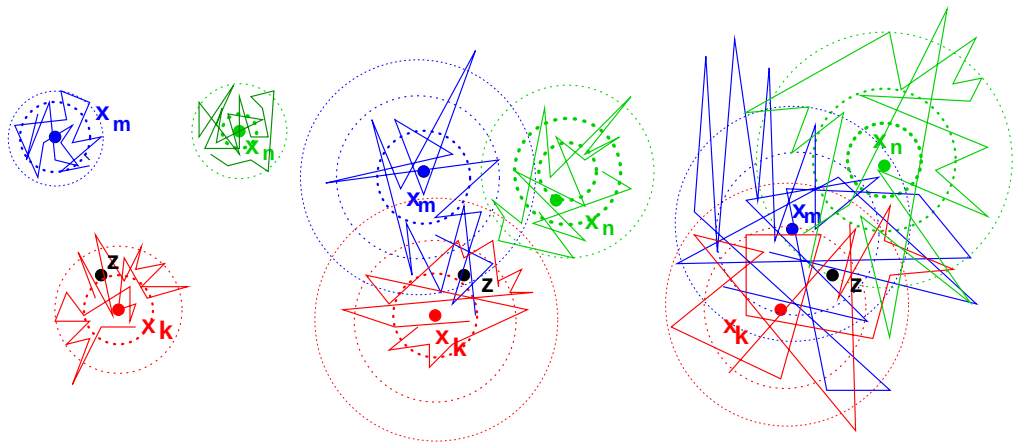

Figure 1: Illustration of temporal evolution of a set of mesoscale elements in the proximity of a fixed location $\boldsymbol{z}$ for three times $t_1 < t_2 < t_3$ shown from the left to right. The dotted lines show isochronals of the presence probability; the solid lines show a possible trajectory of one marked fluid particle the ensemble of which is represented by an m.e.

erties at a point are represented by the intermittency of those represented regions each bringing in its own values of properties and this intermittency is expressed as some weighted sum over the mesoscale elements. Consistently with this idea, a mesoscale element has only a probability of presence at a point but no deterministic position, contrary to other Lagrangian methods where infinitely small particles do have a deterministic position. However, an m.e. is described with single values of velocity and other properties, in which the small-scale fluctuations at scales of m.e. size or smaller are averaged out; these single values are found from evolution equations. In other words, Eulerian statistics of any fluctuating variable is found from Lagrangian statistics of mesoscale elements positions, see figure 1.

One, but not the only, possible way of introducing mesoscale elements in the flow domain would be to consider that an m.e. enters the flow as a flow

parcel representing the time average of inlet flow at a given point or a spatial average of fluid initially, at time t_0, located in the vicinity of a given point if there is no inlet. Regardless of the specific initialisation, let the flow domain V contain an ensemble of N_e mesoscale elements.

Each mesoscale element is attributed a set of time-dependent properties, and even though *sensu stricto* a finite size flow domain must have a distribution of properties, properties of an m.e. are taken as single deterministic values following some evolution equations. For example, instead of considering a temperature pdf within the domain represented by one m.e., this m.e. is associated with one certain value of temperature changing with time because of molecular transfer of heat or heat release from chemical reactions. Each mesoscale element is associated with a location which is the geometrical centre of its region of influence which may be also thought of as the "position" of this m.e. The position of the i-th m.e. is denoted as $\boldsymbol{x}_i(t)$, its temperature as $T_i(t)$ etc. The element age t_i is the time counted since the moment t_i^0 when the i-th m.e. enters the flow domain.

The essential property of an m.e. is its influence on the other locations within the flow domain V: the influence of the i-th m.e. at the point $\boldsymbol{z}$ is given by the time-dependent function $p_i(\boldsymbol{z}, t)$ such that $\int_{t-dt/2}^{t+dt/2} p_i(\boldsymbol{z}, t')dt'$ is the duration, within the interval dt around t, when the point $\boldsymbol{z}$ is occupied by the fluid represented by the i-th m.e. In other words, $p_i(\boldsymbol{z}, t)$ is the indicator function for the fluid represented by the i-th m.e. at the point $\boldsymbol{z}$ at the moment t. Assuming that the interval dt is sufficiently long to average over

it, this means that the average $\bar{g}(\boldsymbol{z},t)$ of a quantity g may be found as:

$$\bar{g}(\boldsymbol{z},t) = \frac{\sum_k^{N_e} g_k(t)\, p_k(\boldsymbol{z},t)}{\sum_j^{N_e} p_j(\boldsymbol{z},t)} \tag{1}$$

and, in particular, the pdf of values taken by a function g at point $\boldsymbol{z}$ at moment t may be found as:

$$P(\hat{g},\boldsymbol{z},t) = \frac{\sum_k^{N_e} \delta(\hat{g} - g_k(t))\, p_k(\boldsymbol{z},t)}{\sum_j^{N_e} p_j(\boldsymbol{z},t)} \tag{2}$$

where $\delta(x)$ is Dirac's delta function and $\hat{g}$ is a particular value taken by the scalar function $g(\boldsymbol{z},t)$. The need for the normalising factor $\sum_j^{N_e} p_j(\boldsymbol{z},t)$ in the denominator comes from the fact that, for a particular application, a coarse m.e. ensemble may not necessarily cover every point of the flow domain providing $\sum_j^{N_e} p_j(\boldsymbol{z}) = 1$ and in such a case the normalised influence function:

$$\tilde{p}_i(\boldsymbol{z},t) = \frac{p_i(\boldsymbol{z},t)}{\sum_k^{N_e} p_k(\boldsymbol{z},t)} \qquad\qquad \bar{g}(\boldsymbol{z},t) = \sum_k^{N_e} g_k(t)\, \tilde{p}_k(\boldsymbol{z},t) \tag{3}$$

is the fraction of the interval dt during which the fluid properties at $\boldsymbol{z}$ are the same as of the i-th m.e. The need for normalisation may also arise when the influence areas of different m.e. overlap in such a way that Eq. 2 produces pdf's with the norm greater than one. The time dependency of $p_k(\boldsymbol{z},t)$ is dropped in what follows to simplify the notation.

If the size of the flow region represented by the i-th m.e. is very small and the turbulence is statistically homogeneous with zero average velocity, then $\boldsymbol{x}_i(t) = \boldsymbol{x}_i^0 = const$ and $p_i(\boldsymbol{z})$ is exactly the pdf of the position of a point particle at the moment t if its initial position is $\boldsymbol{x}_i^0$; this pdf is considered in the analysis of the so-called single-particle diffusion [8, 9]. Even

though an m.e. has a finite size, it shall be assumed here that $p_i(\boldsymbol{z})$ has the functional form similar to the position pdf of the single particle diffusion with the difference that the probability of the spread of the m.e. is taken around the variable $\boldsymbol{x}_i(t)$ rather than a fixed origin:

$$p_i(\boldsymbol{z}) \equiv p_i\left(\boldsymbol{z}; \boldsymbol{x_i}(t), \sigma_i(t)\right) = (2\pi)^{-3/2}\sigma_i^{-3}(t)\, \exp\left(-\frac{\left(\boldsymbol{z}-\boldsymbol{x}_i(t)\right)^2}{2\,\sigma_i^2(t)}\right) \qquad (4)$$

where the width of the distribution $\sigma_i(t)$ has the meaning of the radius of influence of the i-th m.e. Equation 4 is consistent with the assumption of the locally isotropic turbulence as it depends on only the distance $|\boldsymbol{z}-\boldsymbol{x}_i(t)|$ and scalar $\sigma_i(t)$; it is straightforward to generalise equation 4 for the non-isotropic turbulence by introducing second-order tensor σ_i but this derivation is not pursued here.

Attributing a radius of influence $\sigma_i(t)$ to mesoscale element brings into the method a clear separation of scales in that velocity field at the scales smaller than $\sigma_i(t)$ affects its growth while the scales larger than $\sigma_i(t)$ displace the m.e. as a whole:

$$\dot{\boldsymbol{x}}_i(t) = \boldsymbol{u}_i(t) \qquad (5)$$

Herebeneath, the dot means the time derivative of m.e. properties. Growth of the radius of influence $\dot{\sigma}_i(t)$ is determined by the growing dispersion of the m.e. relative to moving $\boldsymbol{x}_i(t)$ and is equivalent to the problem of the relative diffusion of a cloud of contaminant [9, 10, 11]. When σ_i is within the inertial interval, a simple expression follows from the Kolmogorov's hypothesis:

$$\dot{\sigma}_i(t) = \Delta u\left(\sigma_i\right) = C_\sigma\left(\varepsilon(\boldsymbol{x_i}, t)\sigma_i\right)^{1/3} = C_\sigma u' \left(\frac{\sigma_i}{l_t}\right)^{1/3} \qquad (6)$$

where $\varepsilon(\boldsymbol{x_i}, t)$ is the local value of the turbulence dissipation rate, u' is the root-mean-square (rms) velocity fluctuation, l_t is the integral length scale

of turbulence, and C_σ is a universal constant though its exact value is still subject of large uncertainty. Even though equation 6 is written for inertial interval, it coincides with the classical Richardson law of turbulent diffusion experimentally shown to be valid even for very large scales [9] with the constant C_σ being half the value of the constant in Richardson law. For the latter, the recent recommendation [12] is 0.5, hence $C_\sigma = 0.25$. When σ_i increases to the value comparable with the integral length scale l_t, its growth is governed by the simple turbulent diffusion law:

$$\dot{\sigma}_i(t) = C_\sigma u' \left(\frac{\sigma_i}{l_t}\right)^{-1} \tag{7}$$

It may be seen that Eqs. 6 and 7 yield the same growth rate when $\sigma \approx l_t$ and it should be straightforward to devise a simple expression for the power exponential of the $\frac{\sigma_i}{l_t}$ ratio producing a coninuous derivative of the rate of growth for all values of the σ but this is not pursued here: while the notion of the region of influence is cetral in the proposed approach, specific expressions for its extent are not so long as they are compatible with the other assumptions in the theory of homogeneous and isotropic turbulence.

2.2. Eulerian balance equations corresponding to m.e. method

The rate of change of the average transported scalar quantity $\bar{g}(\boldsymbol{z}, t)$ at a fixed location $\boldsymbol{z}$ is expressed, using equation 3, as:

$$\begin{aligned} \partial_t \bar{g}(\boldsymbol{z}, t) \;&=\; \partial_t \textstyle\sum_i g_i(t)\, \tilde{p}_i(\boldsymbol{z}, t) \;=\; \textstyle\sum_i \left[\dot{g}_i\, \tilde{p}_i + g_i(t)\, \partial_t \tilde{p}_i\right] = \\ &\textstyle\sum_i \dot{g}_i\, \tilde{p}_i + \sum_i g_i(t)\, \sum_k \left[\dot{\sigma}_k \partial_{\sigma_k} \tilde{p}_i + \dot{\boldsymbol{x}}_k \cdot \nabla_{\boldsymbol{x}_k} \tilde{p}_i\right] \end{aligned} \tag{8}$$

where the first, second and the third terms describe the effects caused by the processes at the molecular scale, e.g. chemical reactions or molecular

diffusion, and the turbulent convection at the scales inferior and superior to σ, respectively. Using equations from Appendix A.1 and A.3, the above equation may be transformed to a more conventional form:

$$\partial_t \bar{g}(\boldsymbol{z},t) + \nabla_{\boldsymbol{z}} \cdot \overline{\boldsymbol{u}(\boldsymbol{z},t) g(\boldsymbol{z},t)} = S_g + D \tag{9}$$

where the convective flux from the large-scale velocity components $\overline{\boldsymbol{u}g}$, the source term S_g and the turbulent small-scale diffusion D are:

$$\begin{aligned} \overline{\boldsymbol{u}(\boldsymbol{z},t) g(\boldsymbol{z},t)} &= \textstyle\sum_i g_i \dot{\boldsymbol{x}}_i \tilde{p}_i \\ S_g &= \textstyle\sum_i \dot{g}_i \, \tilde{p}_i \\ D &= \textstyle\sum_i g_i \sum_k \dot{\sigma}_k \partial_{\sigma_k} \tilde{p}_i \end{aligned} \tag{10}$$

It is worth noting that the usual turbulent diffusion term $\overline{\boldsymbol{u}'g'}$, i.e. correlation between fluctuations of velocity $\boldsymbol{u}$ and the transported quantity g, is split here between two parts. Further, in contrast to the common expression of the turbulent diffusion in terms of the local flow properties [9], equation 9 is non-local and, for constant turbulence, equation 6 results in $\sigma_k \sim t^{3/2}$, which means that the effective turbulent diffusivity increases with time.

When all mesoscale elements have the same value of the property g, equation 9 reduces to $\nabla_{\boldsymbol{z}} \cdot \overline{\boldsymbol{u}} = 0$; this means that it conserves the mass in incompressible flows where all m.e. have the same density. More general demonstration of mass conservation in the proposed method is demonstrated in the Appendix.

2.3. Mesoscale element dimensions

In order to take the molecular diffusion into account, the dimensions of a mesoscale element should be representative of those of a diffusive layer

formed when a parcel of fluid of a certain composition is brought by the large-scale flow into contact with surrounding with different composition. It is well established, e.g. [13, 14, 15], that turbulent mixing occurs in a large number of layers in which the scalar gradient has one large and two small components and m.e. thickness $\zeta(t)$ is taken as the extent in the direction of the largest scalar gradient component while its length or width $\xi(t)$ is taken as the extent in either of other two dimensions. Essentially, the mesoscale element is taken initially as a cube, $\xi(0) = \zeta(0)$, which is then deformed into a small bent and twisted square patch, one side of which is aligned with the largest component of the scalar gradient and the square sides are normal to it. Conveniently, the initial dimensions are taken in the inertial interval, thus a mesoscale element is a fluid parcel of a constant mass: $m_e = C_m \rho_0 \lambda^3$ where ρ is the fluid density, $\lambda = l_t \cdot Re_t^{-1/2}$ is the Taylor scale of turbulence and C_m is a size-determining constant. Re_t is the turbulent Reynolds number based on the integral length scale. Then for any moment of time t:

$$\xi(t) = \left(\frac{m_e}{\rho(t)\, \zeta(t)} \right)^{1/2} \tag{11}$$

regardless of the shape of m.e. Both experiments, [13, 15] and DNS, e.g.[16], indicate that the m.e. thickness $\zeta(t)$ scales with but (much) larger than the Kolmogorov scale, while its length $\xi(t)$ is much larger than the thickness, going up to sizes comparable with the integral length scale; this explains the particular choice of m.e. dimensions made above.

Evolution of m.e. thickness $\zeta(t)$ is, in principle, determined by four processes: growth caused by molecular diffusion, decrease or increase from compressive or extensive hydrodynamic strain rate, respectively, in ζ direction, and decrease caused by the the strain rate in ξ direction, and the folding of

m.e. There is a clear separation of scales on which these phenomena act, and therefore, at least as a good first approximation, their effects are additive. Folding acts on scales larger than the integral longitudinal length scale [17], much larger than m.e. dimensions, hence its effects may be neglected. Thus:

$$\frac{d\zeta(t)}{dt} = u_{diff} + u_{strain} \tag{12}$$

Acting on its own, in absence of turbulence, molecular diffusion increases the thickness of the diffusive layer arising when two unequal concentrations are brought into contact by the large-scale motion. The speed of thickness increase caused by diffusion may be found assuming that the scalar profile on the m.e. boundary is given by the solution of the diffusion equation for the initial conditions given by the step function. Consider an arbitrary scalar field $Y(\boldsymbol{z}, t)$ with the values normalised between zero and one. The thickness of the diffusive layer is the distance between two arbitrary Y values at the leading $Y \to 0$ and trailing, $Y \to 1$, edge of the diffusive layer. To the constant factor A_d of the order of unity, the rate of thickness growth caused by molecular diffusion may then be found by differentiating the solution of the diffusion equation at a constant Y value:

$$u_{diff} = A_d \left(\frac{\mathcal{D}}{t}\right)^{1/2} \tag{13}$$

where $\mathcal{D}$ is the molecular diffusivity coefficient.

Two components of the hydrodynamic strain field affect the shape of meso-scale element and need consideration: compressive strain rate acting along the ζ direction and normal to it tangential strain rate acting along either of the two ξ directions. These two components of the strain rate are

not independent because of the mass conservation:

$$\frac{1}{\zeta}\cdot\frac{d\zeta}{dt}+\frac{2}{\xi}\cdot\frac{d\xi}{dt}+\frac{1}{\rho}\cdot\frac{d\rho}{dt}\;=\;0 \tag{14}$$

and from this:

$$u_{strain}=-\zeta\left(\frac{2}{\xi}\cdot\frac{d\xi}{dt}+\frac{1}{\rho}\cdot\frac{d\rho}{dt}\right) \tag{15}$$

In homogeneous and isotropic turbulence the scalar gradient tends to align with compressive rather than extensive strain, e.g. see [14] and the discussion and references therein, thus it is sufficient to consider extensive normal strain along ξ direction.

This strain rate is determined by $\Delta u\left(\xi\right)$: the average difference of velocities at the separation ξ, or the square root of the velocity structure function of the second order, [9]. The separation, i.e. the distance between the two points defining the strain rate is taken as ξ, the larger of the two m.e. dimensions. Because, by construction, the m.e. dimensions correspond to the inertial range of turbulence scales, the Kolmogorov self-similarity hypothesis applies:

$$\Delta u\left(\xi\right)=\left(\varepsilon\xi\right)^{1/3}\cdot\tilde{f}\left(\frac{\xi}{l_t}\right)=u'\cdot\left(\frac{\xi}{l_t}\right)^{1/3}\tilde{f}\left(\frac{\xi}{l_t}\right) \tag{16}$$

where $\varepsilon\sim u'^3/l_t$ is the turbulent kinetic energy dissipation, and $\tilde{f}(z)$ is a non-dimensional function universal for all locally isotropic, homogeneous turbulent flows where $Re_t>>1$; this function is related to the longitudinal velocity correlation function $f(z)$, z here is the distance between the two points at which the correlation is considered non-dimensionalised by the integral length scale l_t. While little information is available for $\tilde{f}(z)$, the relationship between f and $\tilde{f}$ may be found considering two extreme separations:

$z \to 0$ and $z \to 1$. In the former case $f \to 1$, while $\tilde{f} \to 0$ as the velocity difference should vanish at zero separation. In the latter case, $f \to 0$ while the average velocity difference should tend to the root-means-square velocity u', hence $\tilde{f} \to 1$. $f(z)$ is the ratio of second moments of velocity, while Δu is the first order moment, thus one should expect that $\tilde{f} \sim f^{1/2}$ The simplest possible relationship satisfying these constraints would be $\tilde{f}(z) = \left(1 - f^{1/2}(z)\right)$.

Using Eqs. 11, 14, one may obtain, to within a factor A_2 of order of unity:

$$u_{strain} = -A_2 \zeta \left[\frac{2\,u'}{l_t^{1/3} \xi^{2/3}} \cdot \left(1 - f^{1/2}(\frac{\xi}{l_t}) \right) \; + \; \frac{1}{\rho} \cdot \frac{d\rho}{dt} \right] \tag{17}$$

This equation should be supplemented with an expression for the longitudinal velocity correlation function $f(z)$; owing to lack of commonly accepted expression suitable for various types of turbulent flows, the following approximation of the measurements of [18] is adopted here:

$$f(z) = J_0 \left(\frac{z}{b} \right) \cdot \exp \left(- \frac{z}{a} \right) \tag{18}$$

where J_0 is the Bessel function of zeroth order. For any value of constant a, $\int_0^\infty f(z)dz = l_t$ if $b = a \cdot (a^2 - 1)^{-1/2}$. Values of $a = 2$, $b = 2/\sqrt{3}$, may be recommended as giving a very good approximation for separations $\lambda \sim z \leq l_t$, see e.g. measurements [18]. It is worth noticing that for separations comparable with or smaller than η, i.e. limit of $z \approx 0$, Eq. 18 requires $a \approx 1$. In the atmospheric turbulence research an alternative expression for the correlation function $f(z)$ due to Frenkiel [19] $f(z) = e^{az} \cos bz$ is used widely, however, Eq. 18 gives significantly more accurate approximation of the measured $f(z)$. It should be finally mentioned that neither Frenkiel expression nor Eq. 18 are accurate at very small separations where the correlation function may

be approximated as $f(z) = 1 - Re_t^- 1 z^2$; however, this approximation, while accurate at $z \approx 0$, is of very poor accuracy at the scales $z \sim \lambda$ or larger which are of interest here. At the present there does not seem to exist an expression for $f(z)$ providing a uniform accuracy over the entire range of turbulence scales.

Finally, the evolution equation for a diffusive layer thickness may be written as:

$$\frac{d\zeta}{dt} = A_1 \left(\frac{\mathcal{D}}{t}\right)^{1/2} - A_2 \zeta \left[\frac{2\,u'}{l_t^{1/3}\xi^{2/3}} \cdot \left(1 - f^{1/2}\left(\frac{\xi}{l_t}\right)\right) + \frac{1}{\rho} \cdot \frac{d\rho}{dt}\right] \qquad (19)$$

where A_1 and A_2 are model constants and f is expressed from Eq. 18. For the inhomogeneous turbulence, the turbulence local properties in Eq. 19 are local and so are the density ρ and the diffusivity $\mathcal{D}$. It is worth noticing that Eq. 19 does not possess a stationary solution owing to the explicit dependency of the first term on the m.e. age t.

3. Equations of evolution of mesoscale element properties

Mesoscale element has fixed mass by construction, thus, in addition to relationships formulated in Section 2, it requires for a complete description of its other properties evolution equations for velocity, two intensive thermodynamic variables and variables describing its chemical composition, e.g. set of mass fractions of species. It has finite dimensions, therefore in principle it requires and additional equation for the angular momentum, as is done in the so-called "asymmetric" or "rational" hydrodynamics, see e.g. [20, 21, 22] and references therein, however, this is left out of consideration in the present formulation. Unlike the usual formulation of Lagrangian methods, see e.g. [23],

where the evolution equations are formulated as partial differential equations involving the initial positions of Lagrangian particles, the evolution equations are formulated here as ordinary differential equations involving m.e. pairwise interactions.

3.1. Meso-element momentum: pressure field

Each act of interaction between two mesoscale elements as derived below conserves momentum. Acceleration of $i-$th m.e. may thus be written as:

$$\dot{\boldsymbol{u}}_{\boldsymbol{i}} = \sum_j \dot{\boldsymbol{u}}_{ij} \tag{20}$$

where $\boldsymbol{u}_{ij}$ is the acceleration caused by its interaction with the $j-$th m.e.

In addition to externally imposed bulk forces, there are two physical agents by which one fluid element affects momentum of other fluid elements: pressure and viscosity, $\dot{\boldsymbol{u}}_{ij} = \dot{\boldsymbol{u}}^p_{ij} + \dot{\boldsymbol{u}}^v_{ij}$; the net acceleration of the element is then obtained as a sum of all pairwise interactions. The superscripts ^{p} and ^{v} refer to the contributions to the total acceleration caused by the pressure field, and viscous forces, respectively. The pressure interaction is considered first; viscous exchange of momentum happening at the contact of two m.e. is considered in the next section. The derivations here concerns only subsonic flows, where the pressure increase arising at one point in flow will induce spherical waves travelling much faster that any fluid parcel. The pressure Π in the front of such spherical wave is inversely proportional to the distance to the point from its centre.

Consider two m.e. the presence pdf of which $p_i(\boldsymbol{z}, t)$ and $p_j(\boldsymbol{z}, t)$ are centred at $\boldsymbol{x}_i$ and $\boldsymbol{x}_j$; the exchange of momentum by pressure waves between them is much faster than their motion, thus their positions may be taken

frozen at $\boldsymbol{x}_i$ and $\boldsymbol{x}_j$. The net pressure force between these m.e. will be $F_p = (\Pi_j - \Pi_i) S_{eff} \frac{\boldsymbol{x}_i - \boldsymbol{x}_j}{(\boldsymbol{x}_i - \boldsymbol{x}_j)}$ where S_{eff} is the cross-sectional area of the m.e. orthogonal to $\boldsymbol{x}_i - \boldsymbol{x}_j$. This force will accelerate of the column of the liquid between and including the two m.e. the mass of which may be taken as $\frac{\rho_i + \rho_j}{2} S_{eff} \, |\boldsymbol{x}_i - \boldsymbol{x}_j|$. By the Second Law of Newton the pressure part of acceleration of either m.e. is

$$\dot{\boldsymbol{u}}^p_{ij} = \dot{\boldsymbol{u}}^p_{ji} = \frac{2(\Pi_j - \Pi_i)}{\rho_i + \rho_j} \frac{\boldsymbol{x}_i - \boldsymbol{x}_j}{(\boldsymbol{x}_i - \boldsymbol{x}_j)^2} \tag{21}$$

3.2. Change of m.e. properties caused by molecular transport

Unlike the above equation, Eq. 21, which describes the rapid momentum change and where the m.e. position may be taken as frozen at the point of the maximum probability of presence, determination of the viscous momentum exchange requires analysis of statistics of m.e. encounters. This is because the molecular transport of momentum, mass and energy acts on scales much smaller than any flow scales, therefore, it may only change of m.e. properties upon a very close contact between two m.e.

The act of interaction between m.e. of which the presence pdf $p_i(\boldsymbol{z}, t)$ and $p_j(\boldsymbol{z}, t)$ are centred at $\boldsymbol{x}_i$ and $\boldsymbol{x}_j$ may happen at any position $\boldsymbol{z}$ within the flow owing to unbounded support of the presence pdf, Eq. 4. Contact, and interaction, between $i - th$ and j-th m.e. at $\boldsymbol{z}$ shall happen if both m.e. are within the distance smaller than the largest dimension of one of them, $\max(\xi_i, \xi_j)$ and, assuming that their motion is uncorrelated, the probability density of the contact at $\boldsymbol{z}$ is the product of the probability density of the i-th element and the probability that j-th m.e. is within the sphere of ξ_i diameter of $\boldsymbol{z}$. The latter is expressed with the help of the theorem of the mean as $\pi/6 \, \max^3(\xi_i, \xi_j) \, p_j(\boldsymbol{z}, t)$.

On the other hand, for a small time interval dt the presence pdf p_i may be interpreted as fraction of dt spent at infinitesimally small vicinity $d\boldsymbol{z}$ of $\boldsymbol{z}$. Therefore, the total time of interaction $p_{ij}dt$ during this time interval between $i-th$ and j-th m.e. is found taking into account that they move and may interact at any point as:

$$p_{ij}(t)dt = \frac{\pi \max^3(\xi_i, \xi_j)}{6} \cdot \int_V p_i(\boldsymbol{z}, t) p_j(\boldsymbol{z}, t) d\boldsymbol{z} \tag{22}$$

Substituting in the above Eq. 4 and performing integration, one obtains:

$$p_{ij}(t)dt = \frac{\max^3(\xi_i, \xi_j)}{12\,(2\pi)^{1/2}} \left(\frac{1}{\sigma_i^2} + \frac{1}{\sigma_j^2}\right)^{\frac{3}{2}} \exp\left(-\frac{(\boldsymbol{x}_i - \boldsymbol{x}_j)^2}{2\left(\sigma_i^2 + \sigma_j^2\right)}\right) \tag{23}$$

Regardless of where m.e. contact and interaction occur, the rate of molecular transfer between two m.e. stays the same as it is determined by the magnitude of small-scale gradients independent, as a first approximation, of the convection by the large-scale velocity field.

A contact interaction of two m.e. will induce one component of the viscous force in direction normal to the contact surface taken here as plane and two tangential components orthogonal to that direction. If to denote $\boldsymbol{b}_m, m = 1 \ldots 3$ the set of the basis vectors of the fixed coordinate system used in Eqs. 5, 10 then the unit vector $\boldsymbol{\tau}_n$ normal to the contact plane in this basis may be written as $\boldsymbol{\tau}_n = (\sin\phi\cos\theta, \sin\phi\sin\theta, \cos\phi)$ and two other vectors forming with it an orthonormal set are: $\boldsymbol{\tau}_{t1} = (-\cos\phi\cos\theta, -\cos\phi\sin\theta, \sin\phi)$ $\boldsymbol{\tau}_{t2} = \boldsymbol{\tau}_n \times \boldsymbol{\tau}_{t1} = (\sin\theta, -\cos\theta, 0)$ where $\phi \in [0, \pi]$, $\theta \in [0, 2\pi]$ are random angles. In isotropic turbulence the normal $\boldsymbol{\tau}_n$ will be uniformly distributed over a sphere, hence the distribution of the angles will be

$$\begin{cases} p_\phi(\hat{\phi}) &= \frac{1}{2}\sin\hat{\phi} \\ p_\theta(\hat{\theta}) &= \frac{1}{2\pi} \end{cases} \tag{24}$$

The viscous force $\boldsymbol{F}_{ij}$ arising at the contact i-th and j-th m.e. is linearly proportional to the area S_c of contact between the m.e. and inversely proportional to the m.e. dimension d_c normal to the plane of contact. The velocity difference inducing the force comes from the difference of the mass velocities $\boldsymbol{u}_j - \boldsymbol{u}_i$ and, in case of a variable density medium, e.g. gas flow with heat exchange, isotropic dilatation velocities $\delta\boldsymbol{u}_{\rho ij} = \boldsymbol{u}_{\rho j} - \boldsymbol{u}_{\rho i} = \delta u_{\rho ij} \sum_m \boldsymbol{b}_m$:

$$\boldsymbol{u}_{\rho i} = -\left(\frac{m_e}{36\pi\rho_i}\right)^{1/3} \frac{\dot{\rho}_i}{\rho_i} \sum_m \boldsymbol{b}_m \tag{25}$$

The dilatation velocity difference will also add a term proportional to the bulk viscosity to the normal force component $F_{nij} = \boldsymbol{F}_{ij} \cdot \boldsymbol{\tau}_n$. The viscous force components may thus be written as:

$$\begin{aligned} F_{nij} &= \frac{S_c}{d_c}\left[\mu_{ij}\left(\boldsymbol{u}_j - \boldsymbol{u}_i + \boldsymbol{u}_{\rho ij}\right)\cdot\boldsymbol{\tau}_n + \left(\eta_{ij} - \frac{2}{3}\mu_{ij}\right)\boldsymbol{u}_{\rho ij}\cdot\boldsymbol{\tau}_n\right] \\ F_{t_1 ij} &= \frac{S_c}{d_c}\left[\mu_{ij}\left(\boldsymbol{u}_j - \boldsymbol{u}_i + \boldsymbol{u}_{\rho ij}\right)\cdot\boldsymbol{\tau}_{t_1}\right] \\ F_{t_2 ij} &= \frac{S_c}{d_c}\left[\mu_{ij}\left(\boldsymbol{u}_j - \boldsymbol{u}_i + \boldsymbol{u}_{\rho ij}\right)\cdot\boldsymbol{\tau}_{t_2}\right] \end{aligned} \tag{26}$$

where μ_{ij} and η_{ij} are dynamic and bulk viscosity, respectively, at the contact. The m-th component of the i-th m.e. acceleration induced by the viscous interaction with j-th m.e. will be determined by the force averaged over the random contact orientation angles ϕ, θ:

$$\dot{u}^v_{mij} = -\dot{u}^v_{mji} = \frac{1}{m_e}\left\langle \boldsymbol{F}_{ij}\cdot\boldsymbol{b}_m\right\rangle_{\phi\theta} = \frac{1}{m_e}\left\langle F_{nij}\boldsymbol{\tau}_n\cdot\boldsymbol{b}_m + F_{t_1 ij}\cdot\boldsymbol{\tau}_{t_1}\cdot\boldsymbol{b}_m + F_{t_2 ij}\cdot\boldsymbol{\tau}_{t_2}\cdot\boldsymbol{b}_m\right\rangle_{\phi\theta} \tag{27}$$

where the angular brackets denote the averaging using the density functions Eq. 24. Substituting Eq. 26 into Eq. 27, one may see that the averaging requires finding pairs $\left\langle\left(\boldsymbol{b}_l\cdot\ \boldsymbol{\tau}_p\right)\left(\boldsymbol{b}_m\cdot\boldsymbol{\tau}_p\right)\right\rangle_{\phi\theta}$ which, after some trivial calcula-

tions, may be found as:

$$\begin{array}{lll} \left\langle (\boldsymbol{b}_1 \cdot \boldsymbol{\tau}_n)^2 \right\rangle_{\phi\theta} = \frac{1}{3} & \left\langle (\boldsymbol{b}_2 \cdot \boldsymbol{\tau}_n)^2 \right\rangle_{\phi\theta} = \frac{1}{3} & \left\langle (\boldsymbol{b}_3 \cdot \boldsymbol{\tau}_n)^2 \right\rangle_{\phi\theta} = \frac{1}{3} \\ \left\langle (\boldsymbol{b}_1 \cdot \ \boldsymbol{\tau}_{t_1})^2 \right\rangle_{\phi\theta} = \frac{1}{6} & \left\langle (\boldsymbol{b}_2 \cdot \ \boldsymbol{\tau}_{t_1})^2 \right\rangle_{\phi\theta} = \frac{1}{6} & \left\langle (\boldsymbol{b}_3 \cdot \ \boldsymbol{\tau}_{t_1})^2 \right\rangle_{\phi\theta} = \frac{2}{3} \\ \left\langle (\boldsymbol{b}_1 \cdot \ \boldsymbol{\tau}_{t_2})^2 \right\rangle_{\phi\theta} = \frac{1}{2} & \left\langle (\boldsymbol{b}_2 \cdot \ \boldsymbol{\tau}_{t_2})^2 \right\rangle_{\phi\theta} = \frac{1}{2} & \left\langle (\boldsymbol{b}_3 \cdot \ \boldsymbol{\tau}_{t_2})^2 \right\rangle_{\phi\theta} = 0 \end{array} \tag{28}$$

and $\left\langle (\boldsymbol{b}_l \cdot \boldsymbol{\tau}_x)\,(\boldsymbol{b}_m \cdot \boldsymbol{\tau}_x) \right\rangle_{\phi\theta} = 0$ if $l \neq m$. Substituting Eq. 28 into Eqs. 27,26, and taking into account the Eq. 23 for the probability of the contact interaction, one obtains:

$$\dot{u}^v_{mij} = \frac{S_c\, p_{ij}(t)}{d_c m_e} \left[\mu_{ij} \left(u_{mj} - u_{mi} + \delta u_{\rho ij} \right) + \frac{1}{3} \left(\eta_{ij} - \frac{2\mu_{ij}}{3} \right) \delta u_{\rho ij} \right] \tag{29}$$

This expression further needs specification of S_c, d_c, and the viscosities at the contact. The contact area S_c is a random quantity which depends on how irregular is the shape of m.e. in contact and their orientation in space. The m.e. dimensions ξ and ζ are orthogonal, so a very simple approach would be to assume that the contact area is proportional to ξ^2 if the unity vectors in ζ direction are aligned, $\boldsymbol{\zeta_i} \cdot \boldsymbol{\zeta_j} = 1$, and $\xi\zeta$ if those vectors are orthogonal, $\boldsymbol{\zeta_i} \cdot \boldsymbol{\zeta_j} = 0$. There are no reasons to assume non-zero correlation between $\boldsymbol{\zeta_i}$, $\boldsymbol{\zeta_j}$ and $\boldsymbol{\tau}_n$, thus the m.e. orientation is random, the average of $\boldsymbol{\zeta_i} \cdot \boldsymbol{\zeta_j}$ is zero, and therefore, the contact area should be proportional to $S_c \sim \xi\zeta$ and, by the same argument, the distance d_c normal to the contact is then proportional to $\xi_i + \xi_j$. Because the viscous flux of momentum goes across the two elements the viscosity of which may be different, e.g. because of their different temperature or composition, the products $S_c\mu_{ij}$ and $S_c\eta_{ij}$ have the meaning of effective conductivities of momentum, therefore, the net conductivity at the contact with the different values of viscosity $\mu_i\xi_i\zeta_i$ and $\mu_j\xi_j\zeta_j$, should, to a factor of order of unity, be $S_c\mu_{ij} = ((\mu_i\xi_i\zeta_i)^{-1} + (\mu_j\xi_j\zeta_j)^{-1})^{-1}$ and, similarly,

$S_c\eta_{ij} = ((\eta_i\xi_i\zeta_i)^{-1} + (\eta_j\xi_j\zeta_j)^{-1})^{-1}$. Finally, using Eqs. 21,29, and taking into account Eq. 11, one may obtain for the m-th component of the total m.e. acceleration, Eq. 20:

$$\begin{aligned} \dot{u}_{mi} \quad &= \frac{1}{\rho_i}\sum_{j\neq i}\left[\frac{\Pi_j-\Pi_i}{\left(\boldsymbol{x_i}-\boldsymbol{x_j}\right)^2}\left(x_{mi}-x_{mj}\right)\right. \\ &\left. +\frac{\xi_j\zeta_j p_{ij}}{(\xi_j+\xi_i)\xi_i}\left[\frac{\mu_i\mu_j(u_{mj}-u_{mi}+\delta u_{\rho ij})}{\mu_i\xi_i\zeta_i+\mu_j\xi_j\zeta_j}+\frac{\omega_i\omega_j\delta u_{\rho ij}}{\omega_i\xi_i\zeta_i+\omega_j\xi_j\zeta_j}\right]\right] \end{aligned} \tag{30}$$

where $\omega = \eta - \frac{2\mu}{3}$ is the second viscosity. Potential of external forces, if present, may be included into Π, e.g. as hydrostatic pressure.

The pressure required in Eq 30 may be found, e.g. using an equation for the energy of $i-$th m.e including effects of composition change, e.g.:

$$E_i = m_e\left(e_i + \frac{\Pi_i}{\rho_i} + \frac{\boldsymbol{u}_i^2}{2} + \sum_s \mu_s n_{si}\right) \tag{31}$$

where e_i is the specific internal energy, $\Pi = \Pi_i^{th} + \Pi_i^h$ is the static pressure, including hydrostatic pressure Π_i^h, the thermodynamic pressure $\Pi_i^{th} = 0$ for incompressible fluid, μ_s is the molar Gibbs energy of $s-$th species and n_{si} is the number of moles of $s-$th species per unit mass of fluid. Differentiation of Eq 31 under different constraints and adding terms accounting for interaction with surrounding, e.g. heat transfer, gives rise to various "energy conservation" equations. The latter may become evolution equations for one of the thermodynamic variables of m.e. if and only if the thermodynamic process followed by fluid elements is known; for example, for a commonly encountered case of an adiabatic flow of compressible gas with chemical reactions, one may obtain:

$$\frac{1+\gamma-\gamma^2}{\gamma}\frac{\dot{\Pi}_i}{\rho_i} + \boldsymbol{u_i}\cdot\dot{\boldsymbol{u}}_{\boldsymbol{i}} = 0 \tag{32}$$

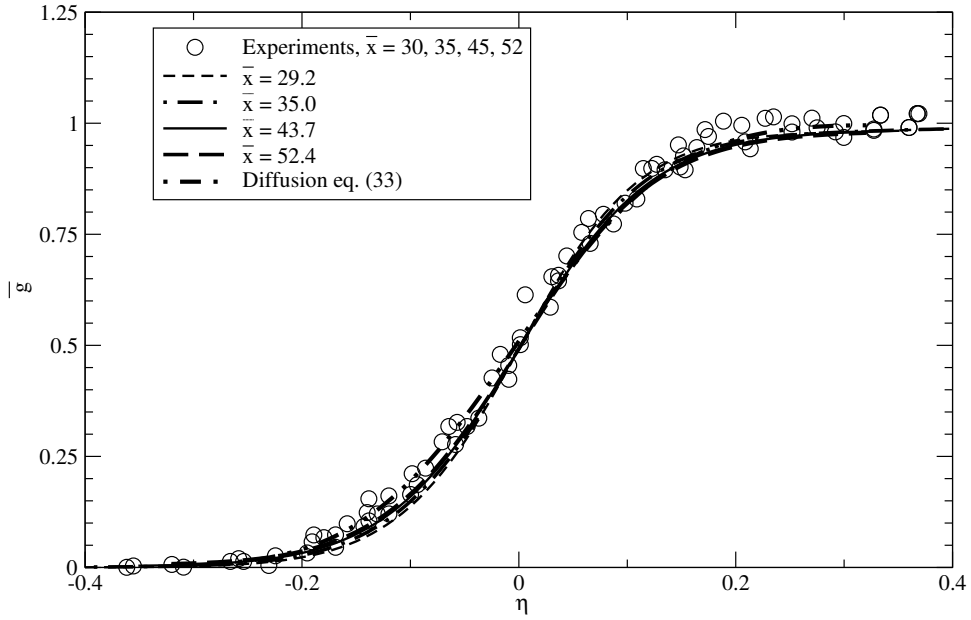

Figure 2: Profiles of the mean scalar vs. self-similar variable η across the mixing layer for the dimensionless distance downstream shown in the legend. Symbols show measurements of [24]. The thick lines show the profiles obtained with the mesoscale elements method, the thin lines - with equation 34.

where γ is the adiabatic index, i.e. the ratio of specific heats at constant pressure and volume processes. Equation 32 would also describe incompressible fluid if to put $\gamma = 1$ reflecting the fact that its specific volume does not depend on pressure.

3.3. Meso-element properties: mass diffusion

Mass diffusion is described similarly to the viscous exchange of momentum considered above. Let g denote a specific quantity, e.g. mass fraction of a chemical compound or enthalpy, then its total amount in i-th m.e. is $m_e g_i(t)$ and let $\mathcal{D}_g$ be the molecular diffusivity of g which may take different values

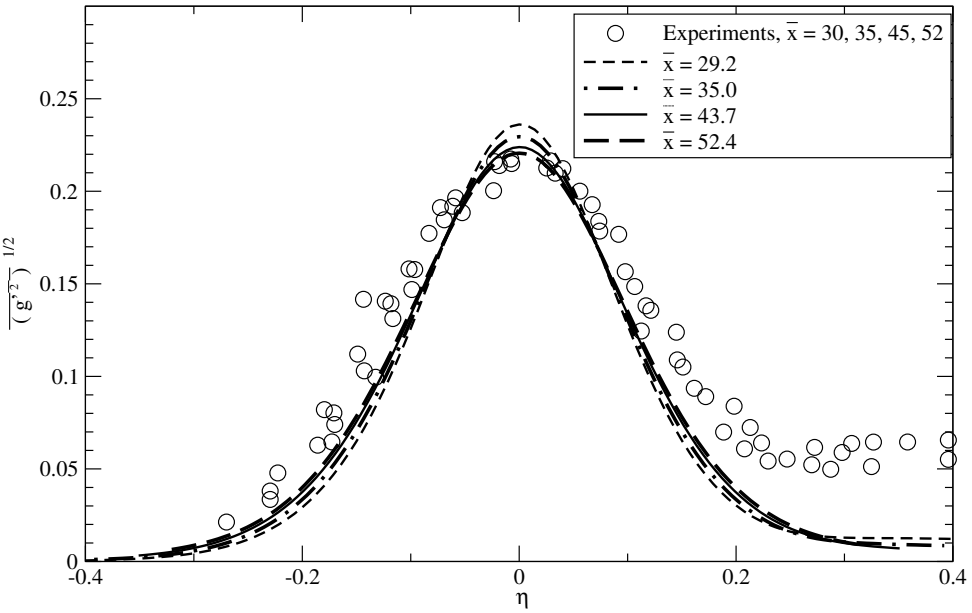

Figure 3: Profiles of the scalar root-mean-square value vs. self-similar variable η across the mixing layer for the dimensionless distance downstream shown in the legend. Symbols show measurements of [24]. The lines show the profiles obtained with the mesoscale elements method.

in different m.e. because of differences in the elements temperature and composition.

Similarly to the viscous flux of momentum, the rate of the molecular transfer of g between i-th and j-th m.e. must be linearly proportional to the area S_c of contact between them, and, as a first approximation, $\mathcal{D}_g$, the molecular diffusivity of g and the difference $g_i - g_j$; it should be inversely proportional to the m.e. dimension normal to the plane of contact taken above as $\xi_i + \xi_j$. For a multi-component mixture, determination of molecular flux of g necessitates consideration of a number of binary diffusion coefficients Ern and Giovangigli [25] but such analysis has not yet been conducted for a turbulent flow, so a single molecular transport coefficient is associated with each variable. It is worth noticing however that the proposed mesoscale formalism may be easily extended to include more complex expressions for the molecular transfer.

From the simplest expression for the amount of quantity exchanged between two m.e. Δg per unit time:

$$\Delta g = \mathcal{D}_g \times (\text{Contact Area}) \times \frac{\rho_i g_i - \rho_j g_j}{(\text{distance normal to contact })}$$

one can see that the product of diffusivity and contact area acts as a certain coefficient of conductivity and it may be different for the two m.e. Because the diffusive flux goes across the two elements with the different values of diffusive conductivities $\mathcal{D}_{gi}\xi_i\zeta_i$ and $\mathcal{D}_{gj}\xi_j\zeta_j$, the net conductivity should be $((\mathcal{D}_{gi}\xi_i\zeta_i)^{-1} + (\mathcal{D}_{gj}\xi_j\zeta_j)^{-1})^{-1}$.

As

$$\Delta g = \frac{d}{dt}(m_e g) = \frac{d}{dt}(\rho\xi^2\zeta g)$$

the molecular transfer contribution to $\dot{g}_i$ in as a sum of pairwise interactions with the entire m.e. set as:

$$\dot{g}_i = -\sum_j \frac{\mathcal{D}_{gi}\,\mathcal{D}_{gj}\xi_j\zeta_j}{\mathcal{D}_{gi}\xi_i\zeta_i + \mathcal{D}_{gj}\xi_j\zeta_j}\ \frac{\rho_i g_i - \rho_j g_j}{\rho_i\xi_i(\xi_i+\xi_j)}\ p_{ij} \tag{33}$$

where p_{ij} is given by equation 23. It is easy to see that equation 33 conserves the total amount of g in the flow:

$$\frac{d}{dt}\left(\sum_i \rho_i\xi_i^2\zeta_i g_i\right) = 0$$

Adding source terms, e.g. due to chemistry, to Eq. 33 provides an evolution equation for $\dot{g}_i$ for any m.e.

4. Illustration of the method: mixing layer

A simulation of a simple turbulent thermal mixing layer has been undertaken as an illustration of the mesoscale elements, this type of flow is commonly used for investigation of turbulent mixing, see e.g. [26, 27]. The simulations correspond to the configuration where the temperature field evolution was measured [24] in freely decaying grid turbulence. In the experiments the thermal mixing layer was initiated by heating half of the turbulence-generating grid rods spaced at distance $M = 4\,cm$. For the simulations, the following parameters were adopted: the flow mean velocity $U = 7.56\,m/sec$, rms velocity of $u' = 0.375\,m/sec$ and integral length scale $l_t = 0.58\,cm$ across a domain the size of which y_1 varied from 8 to 64 l_t. The molecular scalar diffusion was taken as $\mathcal{D} = 0.2cm^2/sec$, $Re_t = 109$.o To reflect the initial non-uniformity of heating, the m.e. scalar values for the heated side, $y \geq y_{0.5}$, were given the initial values sampled from uncorrelated Gaussian distribution

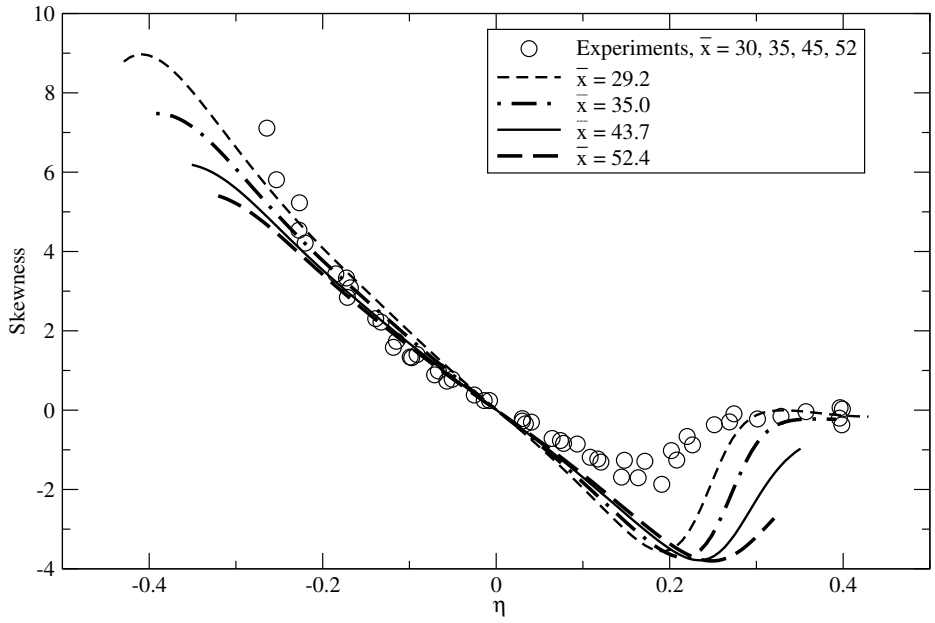

Figure 4: Profiles of the scalar skewness vs. self-similar variable η across the mixing layer for the dimensionless distance downstream shown in the legend. Symbols show measurements of [24]. The lines show the profiles obtained with the mesoscale elements method.

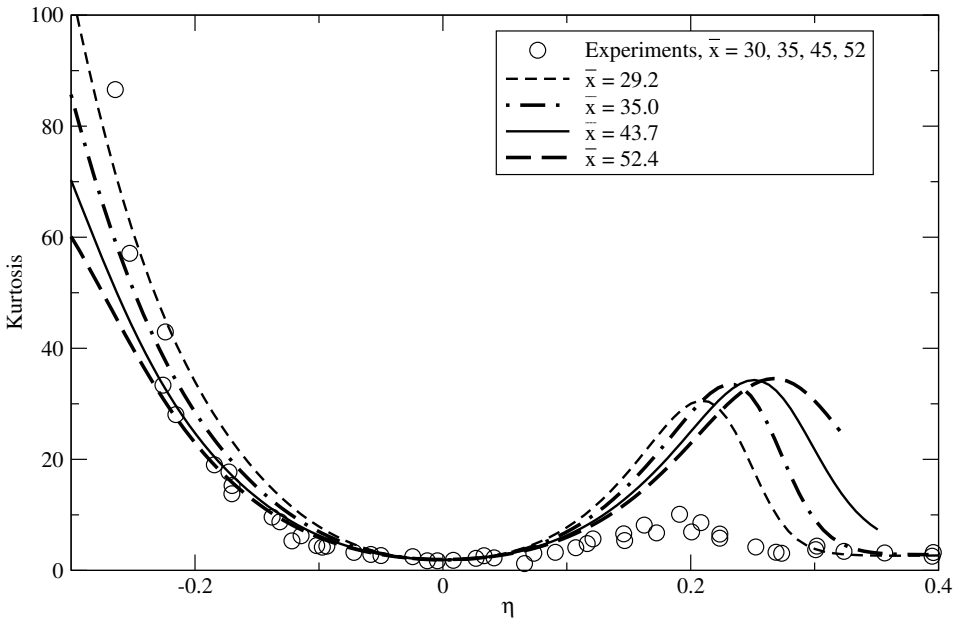

Figure 5: Profiles of the scalar kurtosis vs. self-similar variable η across the mixing layer for the dimensionless distance downstream shown in the legend. Symbols show measurements of [24]. The lines show the profiles obtained with the mesoscale elements method.

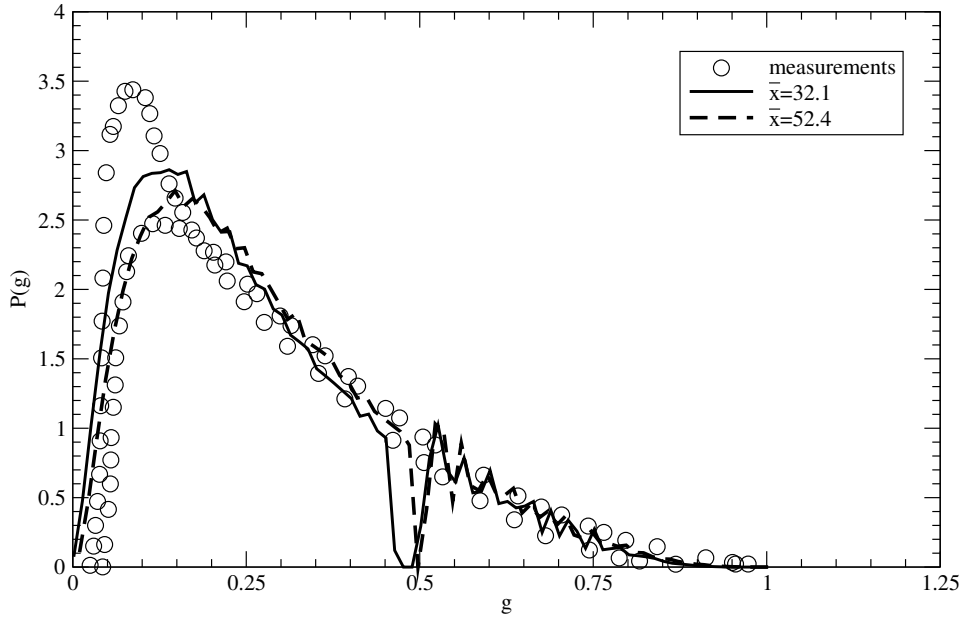

Figure 6: The probability density function of the scalar at positions $\eta = -0.06$ for the dimensionless distance downstream shown in the legend. Symbols show measurements of [24]. The lines show the profiles obtained with the mesoscale elements method.

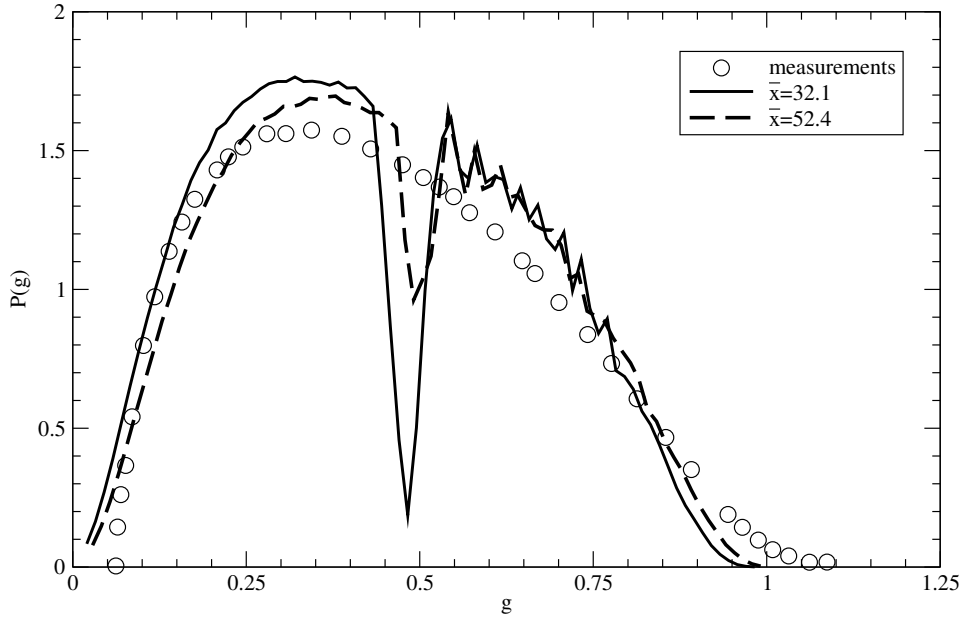

Figure 7: The probability density function of the scalar at positions $\eta = -0.01$ for the dimensionless distance downstream shown in the legend. Symbols show measurements of [24]. The lines show the profiles obtained with the mesoscale elements method.

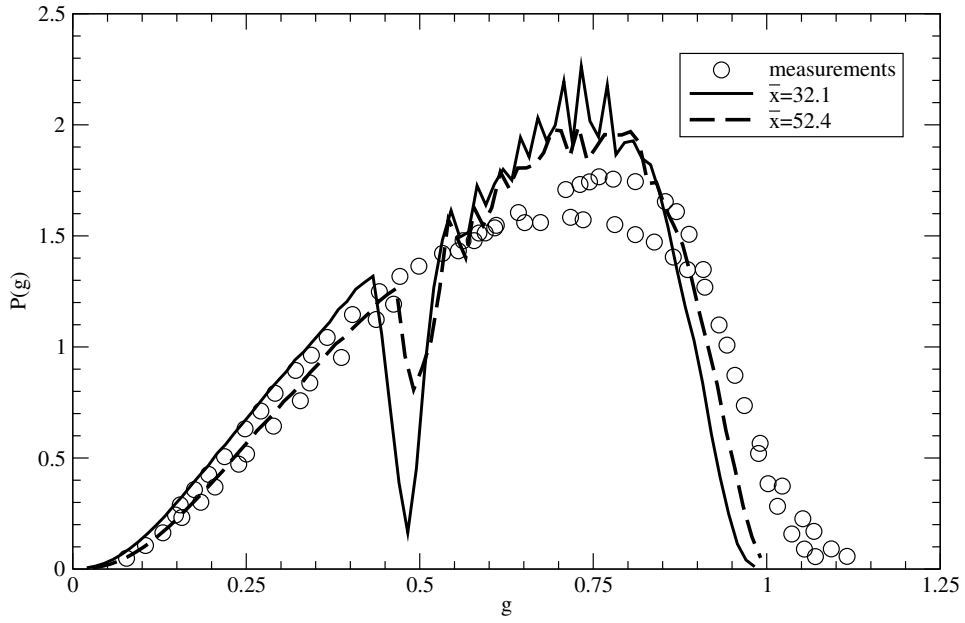

Figure 8: The probability density function of the scalar at positions $\eta = 0.04$ for the dimensionless distance downstream shown in the legend. Symbols show measurements of [24]. The lines show the profiles obtained with the mesoscale elements method.

with the unity mean and the rms value of 0.2; they were initialised as zero value on the cold side $y <_{0.5}$. Thus, the initial mean scalar profile was taken as a step: $g(t=0,y) = \Theta(y - y_{0.5})$ where Θ is the Heaviside function and $y_{0.5}$ is half of the computational domain size. Herebeneath x and y stand for the physical distance downstream and across the boundary layer, respectively. The downstream distance in the mixing layer was translated to the time t in the above equations simply as $x = Ut$.

The set of equations 6, 7, 19, 11, 33 were integrated with respect to time with a second-order explicit Runge-Kutta scheme for number of m.e. placed across the mixing layer; this number varied from 512 to 8192. For all elements, the initial values were taken as $\sigma(t=0) = l_t$, $\xi(t=0) = \zeta(t=0) = \lambda = l_t Re_t^{-1/2}$. The model was implemented in FORTRAN-90 code employing OpenMP parallelisation; GNU FORTRAN was used with intermediate optimisation level. The simulation times on HP Z440 workstation with Intel Xeon E5-1660 with 3.2GHz frequency using 15 out of its 16 cores were under one minute for 512 m.e. and just under 45 minutes for 8192 m.e. No truncation of the influence integrals, Eqs. 4 and 23, to neighbouring mesoscale elements, was attempted, even though it may potentially lead to significant reduction in calculation time.

In addition to the proposed m.e. method, the average scalar values were also calculated with a simple diffusion equation with a constant eddy diffusivity:

$$\partial_t \bar{g}(y,t) = u' l_t \partial^2_{yy} \bar{g}(y,t) \tag{34}$$

supplemented with the boundary conditions $\partial_y \bar{g}(y=0,t) = \partial_y \bar{g}(y=y_1,t) = 0$. This equation is ubiquitous in turbulence modelling and it often describes

well simple self-similar flows. Figure 2 shows the calculated profiles of the mean scalar in comparison with the measurements of [24]. The profiles are given versus the self-similarity variable $\eta = \bar{y}\bar{x}^{-1/2}$ where the distances are non-dimensionalised by the grid spacing $\bar{x} = x/M$, $\bar{y} = y/M$. The measurements clearly show that the mixing layer achieves self-similar state and this behaviour is captured well be the mesoscale elements model, which however does initially show a slower large-scale diffusion caused by the non-steady growing effective diffusivity resulting from Eq. 6.

From inspection of Fig. 3 which shows the scalar root-mean-square value, $g' = \overline{(g - \bar{g})^2}^{1/2}$, one may see that the heated part of the flow studied [24] away from the mixing layer experience decay of the scalar variance similarly to the decay of velocity fluctuations behind the grid. No attempt is made here to capture this decay in the present work: while it is perfectly feasible within the frame of the m.e. method, this would require knowledge of the temperature probability density functions immediately after the heated rods. This explain the discrepancy seen in Fig. 3 for $\eta \geq 0.15$ where the predicted g' is considerably lower than the measured values. Velocity pdf's were measured very closely to the grid in [28] and they show rather complicated transitions from locations immediately past the rods and in between the rods but no information is available for the temperature pdf's in this region. At the same time, the proposed method captures quite well the generation of the scalar variance in the region of the non-zero average scalar derivatives and subsequent reduction of variance due to the action of molecular transfer; this behaviour is described by the present model qualitatively and quantitatively correctly.

Higher order moments, such as skewness $S = \overline{(g-\bar{g})^3} g'^{-3}$ and kurtosis $K = \overline{(g-\bar{g})^4} g'^{-4}$ are sensitive to the shape of the probability distribution and, owing to this, their prediction presents a stringent test for turbulence modelling [26, 27]. Figures 4 and 5 show the calculated profiles of the skewness and kurtosis across the mixing layer in comparison with the measurements of [24]. One may see that within the mixing layer, that the model captures well the observed convergence of these moments to a self-similar state and on the heated side away from the mixing layer, while the magnitude of these moments is over-predicted on the mixing layer boundary on the heated side. It is interesting to notice that this discrepancy is also shared by the direct numerical simulations of [26]. Considerably higher than the observed values of the kurtosis together with larger negative values for skewness mean that the model over-predicts both the frequency and the magnitude of the cold air excursions on the "hot" side, $y \geq 0$, of the mixing layer while an excellent agreement on the "cold" side means that the predictions of the excursions of the heated air are accurate. This means that the velocity pdf deviates from Gaussian distributions on the "hot" side; m.e. simulations of joint velocity-scalar probability distribution should capture this but are left for the subsequent work.

Figures 6, 7, 8 show the evolution of the scalar probability density function $P(g)$ across the mixing layer. The first comment is that, while the shape of the predicted scalar pdf compares well with the measurements across the layer the simulations show low probability at the layer mid-position, in a very narrow region, and this is an artefact of the simulations dependent on the number of elements. The magnitude of this non-physical drop of $P(g)$ near

$g \approx 0.5$ is larger for smaller number of m.e. and is progressively decreased where larger number, i.e. higher spatial resolution is used. Another effect of smaller m.e. number across the mixing layer is increased unevenness of the scalar pdf on the "hot" side, $g \geq 0.5$ seen in Figs. 6, 7, 8. Yet, despite these two shortcomings, one may see that the scalar pdf's are predicted in a very good agreement across the entire mixing layer thus lending support to the model formulation presented here. In particular, there is a good agreement in the probability tails, i.e. large deviations from the mean; one may also see that the over-prediction of kurtosis and skewness on the "hot" side seen in Figs. 4 and 5 is caused by a relatively small difference between predicted and measured scalar pdf near $g \approx 1$. It is perhaps worth noticing that derivation of transport equations for a third or fourth order moment in Eulerian framework would involve fourth or fifth order correlations, respectively, of which little is known, and to the author's best knowledge this has not even been attempted. The pdf shape shown in Figs. 6, 7, 8 is sensitive to the magnitude of the molecular diffusivity; suffice to say that for the black-and-white mixing, $\mathcal{D}_g = 0$, the pdf is strictly bimodal, $g'^2 = \bar{g}(1-\bar{g})$ while S and K are infinite: the simulations (results not shown here) reproduce this to accuracy proportional to the square of the deployed number of m.e, e.g. $S \approx N^2$ etc.

A natural further assessment of the proposed mesoscale elements method will be its application to chemically reacting flows, in particular for frequently encountered cases where the chemical reactions occur in thin fronts and where there is a very strong dependency on the molecular transport coefficients.

5. Conclusions

This work puts forward a new approach to description of a turbulent flow introducing Lagrangian elements of finite mass which are contribute to flow statistics over a certain region of influence. These elements, named mesoscale elements, or m.e., undergo deformation by fluctuating strain field, and this deformation determines the rate of molecular transport between them. These are central points of this new approach. It may be viewed as Lagrangian equivalent of the so-called "Large-Eddy Simulations" gaining prominence in Eulerian fluid dynamics.

This work formulates expressions, either algebraic or differential, for the new quantities associated with these mesoscale elements. In particular, the probability of the m.e. presence at a point is presumed as a Gaussian distribution, the parameters of which obey simple ordinary differential equations, Eqs. 4, 5, 6. The molecular transport is expressed as effect of pairwise m.e. interactions and it is shown that these interactions satisfy the relevant conservation laws. The derivations in the present work are made for the m.e. dimensions of which lay in the inertial interval of the turbulence scales and make consistent use of Kolmogorov's theory of homogeneous and isotropic turbulence. The proposed approach achieves quite clear separation of scales between the molecular transport, i.e. pairwise interactions, at the microscale, and large-scale turbulent diffusion encapsulated in Eqs. 4, 6 and convection by the average velocity field. It is perhaps worth stating, that the mesoscale approach is quite general in the sense that any of the proposed equations for the m.e. properties may be refined, improved or otherwise altered within the same framework; clearly any such modification must be consistent with the

central ideas of an element of finite mass exerting non-local influence on the turbulent flow statistics.

This first application of the mesoscale elements method to a simple mixing layer produced qualitatively correct results in good agreement with the measurements; this concerns not only the mean and root-mean square scalar values, but also the probability distributions and higher order moments. The subsequent work should address the viability of the method for the reacting flows, in particular for frequently encountered cases where the chemical reactions occur in thin fronts where the strong dependency on the molecular transport will allow a better assessment of requirements for the numerical resolution, number of elements required for a given level of accuracy and other details of the method implementation.

References

[1] S. B. Pope, Annu. Rev. Fluid Mech. 26 (1994) 23–63.

[2] J.-P. Minier, S. Chibbaro, S. Pope, Physics of Fluids 26 (2014).

[3] D. H. Rowinski, S. Pope, Combustion Theory and Modelling 15 (2011) 245 – 266.

[4] C. Dopazo, in: P. Libby, F. Williams (Eds.), Turbulent Reacting Flows, Acad. Press, London, 1994, pp. 375–473.

[5] C. Dopazo, L. Cifuentes, J. Hierro, J. Martin, Flow Turbulence Combust. 96 (2016) 547–571.

[6] A. Lipatnikov, J. Chomiak, Combust. Sci. and Tech. 137 (1998) 277–298.

[7] A. Lipatnikov, J. Chomiak, Progr. Energy Comb. Sci, 31 (2005) 1–73.

[8] G. K. Batchelor, Mathematical Proceedings of the Cambridge Philosophical Society 48(2) (1952) 345–362.

[9] A. Monin, A. Yaglom, Statistical hydromechanics, Izd-vo "Nauka", Moscow, 1965.

[10] P. Chatwin, P. Sullivan, Journal of Fluid Mechanics 91 (1979) 337–355.

[11] G. K. Batchelor, Australian Journal of Scientific Research, Series A: Physical Sciences 2 (1949) 437–450.

[12] G. Gioia, G. Lacorata, E. M. Filho, A. Mazzino, U. Rizza, Boundary-Layer Meteorology 113 (2004) 187–199.

[13] K. Buch, W. Dahm, J. Fluid Mech. 364 (1998) 1–29.

[14] H. Abe, R. Antonia, H. Kawamura, J. Fluid Mech. 627 (2009) 1–32.

[15] L. Su, N. Clemens, J. Fluid Mech. 488 (2003) 1–29.

[16] N. Kornev, V. Zhdanov, E. Hassel, Int. J. Heat Fluid Flow 29 (2008) 665–674.

[17] A. Burluka, Diffusion layer thickness in turbulent flow, 2018. Submitted to Int. J. Heat and Fluid Flow.

[18] A. Burluka, A. El-Dein Hussin, Z.-Y. Ling, C. Sheppard, Experimental Thermal and Fluid Science 43 (2012) 13–22.

[19] F. Frenkiel, Proc. USA Nat. Acad. Sci 38 (1952) 509–515.

[20] V. Nikolaevskii, Journal of Applied Mathematics and Mechanics 34 (1970) 482 – 493.

[21] M. Iovieno, D. Tordella, Phys. Fluids 14 (2002) 2673 – 2682.

[22] V. A. Babkin, V. N. Nikolaevskii, Journal of Engineering Physics and Thermophysics 84 (2011) 430–439.

[23] A. Bennet, Lagrangian Fluid Dynamics, Cambridge Univ. Press, Cambridge, UK, 1 edition, 2006.

[24] J. LaRue, P. Libby, Phys Fluids 24 (1981) 597–603.

[25] A. Ern, V. Giovangigli, in: Lecture Notes in Physics, New Series Monographs, volume 24, Heidelberg: Springer-Verlag, 1994.

[26] S. de Bruyn Kops, J. Riley, Phys Fluids 12 (2000) 185–192.

[27] S. B. Pope, Physics of Fluids 25 (2013) 110803.

[28] Jayesh, Z. Warhaft, Phys. Fluids A, 4 (1992) 2292–2307.

Appendix A.

As the m.e influence function p_i depends only on the difference $|\boldsymbol{z} - \boldsymbol{x}_i(t)|$, $\nabla_{\boldsymbol{x}_k} p_k = -\nabla_{\boldsymbol{z}} p_k$. For the normalised m.e. "presence" pdf $\tilde{p}_i$ given by equation 3, one may write:

$$\begin{aligned}
\partial_{\sigma_k}\tilde{p}_i = &\quad -\tilde{p}_i \tfrac{\partial_{\sigma_k} p_k}{\sum_k p_k} \qquad \nabla_{\boldsymbol{x}_k}\tilde{p}_i = \quad -\tilde{p}_i \frac{\nabla_{\boldsymbol{x}_k} p_k}{\sum_k p_k} \qquad k \neq i \\
\partial_{\sigma_i}\tilde{p}_i = &\quad (1-\tilde{p}_i) \tfrac{\partial_{\sigma_i} p_i}{\sum_k p_k} \qquad \nabla_{\boldsymbol{x}_i}\tilde{p}_i = \quad (1-\tilde{p}_i) \frac{\nabla_{\boldsymbol{x}_i} p_i}{\sum_k p_k} \\
\nabla_{\boldsymbol{z}}\tilde{p}_i = &\quad \tfrac{1}{\sum_k p_k} \left(\nabla_{\boldsymbol{z}} p_i - \tilde{p}_i \tfrac{\sum_k \nabla_{\boldsymbol{z}} p_k}{\sum_k p_k} \right)
\end{aligned} \tag{A.1}$$

Using these relationships, further two useful identities may easily be shown:

$$\sum_i \left(\sum_k \dot{\sigma}_k \partial_{\sigma_k} \tilde{p}_i \right) = 0 \qquad \sum_i \left(\sum_k \dot{\boldsymbol{x}}_k \nabla_{\boldsymbol{x}_k} \tilde{p}_i \right) = 0 \tag{A.2}$$

These two expressions may be in particular be used to demonstrate that m.e. equations satisfy mass conservation in incompressible case regardless of specific expressions for $\dot{\sigma_k}$ and $\dot{\boldsymbol{x}_k}$.

Derivation of the Eulerian balance equations require expression of the derivatives of the averaged quantities in terms of the m.e. sums, e.g:

$$\nabla_{\boldsymbol{z}} \bar{g}(\boldsymbol{z}, t) = \nabla_{\boldsymbol{z}} \left(\sum_i g_i(t) \tilde{p}_i \right) = \sum_i g_i \nabla_{\boldsymbol{z}} \tilde{p}_i \tag{A.3}$$

It is obvious that in the m.e. method the averaging and spatial differentiation are commutative, but differentiation with respect to time automatically includes advection terms.

The final remark concerns often required integration of an average flow property over the entire flow domain, e.g. the volume integral of the density giving the total mass of the fluid is often used to verify the mass conservation. Consider a fixed Eulerian grid, i.e. a set of fixed points $\boldsymbol{z}_l, l = 1 \ldots N_p$ such that the union of small volume elements dV_l centred on them covers the entire flow domain. Then any integral over the flow domain V_f may be approximated as the finite sum:

$$\int_{v_f} d\boldsymbol{z} \overline{f(g(\boldsymbol{z}, t)} = \sum_l^{N_p} dV_l \overline{f(g(\boldsymbol{z}_l, t)}$$

On the other hand $\overline{f(g(\boldsymbol{z}_l, t)} = \sum_i g_i(t) \tilde{p}_i \left(\boldsymbol{z}_l, t \right)$. Thus:

$$\int_{v_f} d\boldsymbol{z} \overline{f(g(\boldsymbol{z}, t)} = \sum_l^{N_p} dV_l \sum_i g_i(t) \tilde{p}_i \left(\boldsymbol{z}_l, t \right) = \sum_i g_i(t) \sum_l^{N_p} dV_l \tilde{p}_i \left(\boldsymbol{z}_l, t \right) = \sum_i g_i(t)$$

as the sum over the grid is simply the total probability of the presence of i-th m.e. somewhere in the flow and it is unity by virtue of Eq. 3.